Colloids and Surfaces B: Biointerfaces 136 (2015) 900–907

Contents lists available at ScienceDirect

Colloids and Surfaces B: Biointerfaces

journal homepage: www.elsevier.com/locate/colsurfb

Mucoadhesive thermo-responsive chitosan-*g*-poly(*N*-isopropylacrylamide) polymeric micelles *via* a one-pot gamma-radiation-assisted pathway

Alejandro Sosnik[a,*], Julieta C. Imperiale[b,c], Brenda Vázquez-González[d], Maya Menaker Raskin[a], Franklin Muñoz-Muñoz[e], Guillermina Burillo[d], Gerardo Cedillo[d], Emilio Bucio[f]

[a] *Laboratory of Pharmaceutical Nanomaterials Science, Department of Materials Science and Engineering, Technion-Israel Institute of Technology, Technion City 3200003, Haifa, Israel*
[b] *Department of Pharmaceutical Technology, Faculty of Pharmacy and Biochemistry, University of Buenos Aires, Buenos Aires, Argentina*
[c] *National Science Research Council (CONICET), Buenos Aires, Argentina*
[d] *Departamento de Química de Radiaciones y Radioquímica, Instituto de Ciencias Nucleares, Universidad Nacional Autónoma de México, México DF, Mexico*
[e] *Centro de Nanociencias y Nanotecnología, Universidad Nacional Autónoma de México, Tijuana-Ensenada, Mexico*
[f] *Instituto de Investigaciones en Materiales, Universidad Nacional Autónoma de México, México DF, Mexico*

ARTICLE INFO

Article history:
Received 31 July 2015
Received in revised form 20 October 2015
Accepted 26 October 2015
Available online 30 October 2015

Keywords:
Thermo-responsive chitosan-*g*-poly(*N*-isopropylacrylamide) copolymers
Gamma-radiation-assisted free radical polymerization
Mucoadhesive polymeric micelles
Indinavir free base encapsulation

ABSTRACT

Thermo-sensitive graft copolymer amphiphiles of chitosan (CS) and poly(*N*-isopropylacrylamide) (PNiPAAm), CS-*g*-PNIPAAm, were successfully synthesized by a catalyst-less one-pot gamma (γ)-radiation-assisted free radical polymerization at three different radiation doses: 5, 10 and 20 kGy. The chemical structure of the copolymers was confirmed by FTIR and solid-state ^{13}C NMR and the grafting extent by ^{1}H NMR and gravimetric analysis. In general, the higher the dose, the smaller the grafting due to the more significant NiPAAm homopolymerization. Due to the grafting of poly(NiPAAm) blocks, aqueous solutions of the different copolymers underwent a sharp transition upon heating above 32 °C, the characteristic lower critical solution temperature (LCST) of poly(NiPAAm). Then, the critical micellar concentration (CMC), the size and size distribution and the zeta-potential were characterized by dynamic light scattering (DLS) and the polymeric micelles visualized in suspension and quantified by Nanoparticle Tracking Analysis (NTA), at 37 °C. CMC values were in the 0.0012–0.0025% w/v range and micelles displayed sizes between 99 and 203 nm with low polydispersity (<0.160) and highly positive zeta-potential (>+15 mV) that suggested the partial conservation of the amine groups upon NiPAAm grafting. Consequently, polymeric micelles displayed the intrinsic mucoadhesiveness of CS, as established *in vitro* by the mucin solution assay. Finally, the encapsulation capacity of the micelles was assessed with the highly hydrophobic protease inhibitor antiretroviral indinavir free base (IDV). Polymeric micelles led to a significant 24-fold increase of the aqueous solubility from 63 μg/mL to 1.45 mg/mL, a performance remarkably better than different poly(ethylene oxide)-*b*-poly(propylene oxide) block copolymers assessed before. Overall results highlight the potential of this nanotechnology platform to expand the application of polymeric micelles to mucosal administration routes.

1. Introduction

Polymeric micelles are one of the most versatile nanocarriers for encapsulation, delivery and targeting of poorly water-soluble drugs [1,2], though owing to a number of structural disadvantages such as weak interaction with mucosal tissues, their implementation by non-parenteral administration routes has been much more constrained than by the parenteral ones [3,4]. For instance, the only polymeric micelle-based drug delivery systems that reached advanced clinical trials or the clinics are for the intravenous therapy of cancer [5,6]. Aiming to overcome this limitation, different synthetic pathways have been explored to confer amphiphilicity to polysaccharides and other multifunctional mucoadhesive polymers [7].

* Corresponding author.
E-mail addresses: sosnik@tx.technion.ac.il, alesosnik@gmail.com (A. Sosnik).

http://dx.doi.org/10.1016/j.colsurfb.2015.10.036
0927-7765/

Chitosan (CS) is a pH-dependent polycationic polymer obtained by deacetylation of chitin that owing to its very good biocompatibility, biodegradability, and non-toxicity has been classified into the "Generally Recognized as Safe" (GRAS) excipient category of the US-FDA [8], gaining a preponderant place in the biomedical field [9–12]. In addition, CS is one of the most versatile and efficient mucoadhesive polymers due to the exhibition of several complementary mucoadhesion mechanisms [13,14]. Another striking feature of CS as a platform for mucosal nano-drug delivery is the ability to reversibly open tight junctions in different epithelia [15,16], a phenomenon that increases the apical-to-basolateral permeability of nanomaterials across epithelial tissues such as the gastrointestinal, the nasal and the pulmonary ones [17,18].

One of the most straightforward methods to convert CS into an amphiphile is the conjugation of fatty acids [7]. However, the chemical flexibility to fine-tune the hydrophilic–lipophilic balance (HLB) is relatively limited. Another approach that is gaining impulse is the graft polymerization of hydrophobic blocks employing CS as a molecular template and capitalizing on the presence of reactive hydroxyl and amine side-chain groups [7,19]. In this framework, different chemistries and technologies that increase monomer conversion rates and minimize the use of catalysts is of great interest [20].

Gamma (γ)-radiation has been extensively investigated as a one-step and relatively clean method for the graft radical polymerization of a broad spectrum of monomers with better yields than those achieved by chemical and UV-initiated reactions [21–23]. In general, the graft-modified polysaccharides were used for the production of microscopic and macroscopic hydrogels [24–26]. Conversely, this technology has not been previously investigated for the hydrophobic modification of polysaccharides and the production of self-assembly polymeric nanomaterials (*e.g.*, polymeric micelles) envisioned for drug delivery.

Poly(*N*-isopropylacrylamide) (PNIPAAm) is one of the most popular thermo-responsive polymeric biomaterials [27–29]. PNIPAAm aqueous solutions exhibit a lower critical solution temperature (LCST) between 30 and 35 °C that can be tuned by copolymerization or blending with other monomers. At temperatures lower than the LCST, PNIPAAm has a hydrophilic behavior, whereas at temperatures above it, it undergoes dehydration and adopts a collapsed hydrophobic state [30–32]. This reversible phase transition has been extensively exploited in drug delivery and tissue engineering [30–32].

On this conceptual background, in the present work, we investigated the grafting of PNIPAAm blocks to a CS backbone *via* a catalyst-less one-pot γ-radiation-assisted reaction to confer the polysaccharide thermo-responsive self-assembly properties and produce mucoadhesive polymeric micelles under physiological conditions. Employing a ^{60}Co γ-source with a dose rate of 12.06 kGy/h and radiation doses of 5–20 kGy, reactions were completed within 25–100 min. The smaller the dose, the higher the PNIPAAm grafting due to less NiPAAm homopolymerization. Amphiphiles self-assembled at relatively low concentrations in the 0.0012–0.0025% w/v range and formed polymeric micelles with sizes between 100 and 200 nm and positively-charged surface that led to agglomeration in the presence of soluble mucin. Finally, the polymeric micelles displayed a good encapsulation capacity for the poorly water-soluble protease inhibitor antiretroviral indinavir free base (IDV), opening new promising avenues for the improved mucosal delivery of hydrophobic drugs.

2. Experimental

2.1. Materials

Low molecular weight CS (95.5% deacetylation, 39 cP, 1% w/w in 1% acetic acid at 25 °C) and mucin from porcine stomach (type III) were purchased from Sigma–Aldrich (St. Louis, MO, USA) and used as received. NiPAAm (Sigma–Aldrich) was purified by recrystallization in hexane/toluene (50/50, v/v) at 30 °C. IDV was isolated from commercial Crixivan® (indinavir sulfate) 400 mg capsules (Merck & Co., Inc., Kenilworth, NJ, USA) as described elsewhere [33]. Ammonium hydroxide, toluene, hexane and ethanol were from JT Baker (Mexico City, Mexico), and triethylamine and acetonitrile (chromatographic grade) from Sintorgan (Buenos Aires, Argentina).

2.2. One-pot γ-radiation-assisted synthesis of the graft copolymers

CS (0.17 g) was dissolved in aqueous solution of NIPAAm (0.166 M; 10 mL), this solution placed in a glass ampoule and degassed by bubbling argon (20 min). Then, the ampoule was sealed and irradiated with a ^{60}Co γ-source (Gammabeam 651-PT, Nordion International Inc., Ottawa, Canada) with an activity of 63,000 Ci at a dose rate of 12.06 kGy/h and radiation doses of 5, 10 and 20 kGy; these doses representing irradiation times of 25, 50 and 100 min, respectively. Reaction crudes were washed with an ammonium hydroxide solution/ethanol (3/7 v/v) mixture, filtered, washed again water and dried under vacuum at room temperature to constant weight. The copolymers obtained with radiation doses of 5, 10 and 20 kGy are named CS-*g*-PNIPAAm-05, CS-*g*-PNIPAAm-10 and CS-*g*-PNIPAAm-20, respectively. PNIPAAm homopolymer was prepared following a similar protocol and doses of 5 and 20 kGy, though without the addition of CS to the reaction mixture. This polymer and pristine CS were used along the work as controls.

2.3. Copolymer characterization

2.3.1. Nuclear magnetic resonance (NMR) spectroscopy

^{1}H NMR spectra of the different copolymers were recorded in a 400-MHz Bruker® Avance III High Resolution spectrometer (Bruker BioSpin GmbH, Rheinstetten, Germany) and SpinWorks 4.0 software (Manitoba University, MB, Canada) using D_2O with 5% v/v acetic acid-d_4 (Sigma–Aldrich) as solvent and 5% w/v solutions. Chemical shifts are reported in ppm using the signal of H_2O (4.79 ppm) as internal standard. To determine the weight percent of NiPAAm in the copolymers (%NIPAAm), a calibration curve was prepared using physical mixtures of NIPAAm: CS with weight ratio of 5:1, 2:1 and 1:1 (R^2 = 0.9935). The ratio between the integrations of the signal at 3.1 ppm due to CS and at 1.1 ppm due to NIPAAm was calculated and interpolated for each product in the calibration curve to determine the relative weight contents in the copolymer. ^{13}C CP/MAS NMR spectra of CS and the three copolymers were recorded on a Bruker Avance 400 MHz Spectrometer (Bruker BioSpin GmbH) in solid state at a frequency of 100 MHz. Samples (~250 mg) were placed in a zirconia rotor (4 mm), the spinning rate was set at magic-angle spinning of 5 kHz and ^{13}C chemical shifts were referenced with an external standard of glycine.

2.3.2. Attenuated total reflectance Fourier transform infrared (ATR-FTIR) spectroscopy

ATR-FTIR spectra of the graft copolymers, pristine CS and NiPAAm were recorded from 650 to 4000 cm^{-1} (16 scans) in a PerkinElmer Spectrum 100 (PerkinElmer Cetus Instruments, Norwalk, CT, USA) equipped with a Universal ATR sampling accessory

and a diamond tip. Baseline subtraction was carried out using the spectrum software supplied with the equipment.

2.3.3. X-ray diffraction

X-ray diffraction patterns of each copolymer were recorded at room temperature with Cu Kα radiation in a Rigaku ULTIMA-IV diffractometer in the θ–2θ configuration (Rigaku Corp., Tokyo, Japan). The diffraction intensity was measured in the 2θ scattering range between 5 and 70°, with a 2θ step of 0.02° and 1.2 s per point.

2.3.4. Lower critical solution temperature (LCST) and glass transition temperature (T_g)

To determine the LCST of the thermo-responsive copolymers, samples were weighed in 40 μL Al-crucibles pans, wetted by the addition of a 50–100 μL of water, sealed and heated in a differential scanning calorimeter (DSC 2010 calorimeter, TA Instruments) from 20 to 100 °C (heating rate of 1 °C/min) under N_2 atmosphere. The onset point of the first endothermal peak was determined by intersecting two tangent lines from the baseline and the slope of the endothermal peak and used to establish the LCST. Then, dry samples were ran between 25 and 300 °C (10 °C/min) and the T_g of PNiPAAm blocks determined.

2.3.5. Thermal stability

The thermal decomposition of the different copolymers, pristine CS and PNiPAAm was analyzed between 25 and 800 °C (heating rate = 10 °C/min) under a nitrogen atmosphere in a TGA Q50 (TA Instruments, New Castle, DE, USA). The char yield (%) is the weight percent of the original sample mass that remains after heating to 800 °C under N_2 atmosphere.

2.4. CS-g-PNIPAAm polymeric micelles

2.4.1. Critical micelle concentration (CMC)

A stock solution (0.5% w/v) was prepared by dissolving the graft copolymer in acetic acid solution 2% v/v under vigorous magnetic stirring at 8 °C. Once the copolymer dissolved, the pH was adjusted to 5.50 with NaOH 1N and the volume complete with water. Then, water dilutions were prepared in the 0.00005–0.1% w/v concentration range, samples incubated at 37 °C (12 h) and the intensity of the scattered light (expressed in kilo counts per second) measured by Dynamic Light Scattering (DLS, Zetasizer Nano-ZS, Malvern Instruments, Malvern, UK). The instrument is provided with 4 mW He–Ne laser (λ = 633 nm), digital correlator ZEN3600 and a Non-Invasive Back Scatter (NIBS®) technology. Measurements were carried out at a scattering angle of 173° to the incident beam and data analyzed using CONTIN algorithms (Malvern Instruments). Data of each dilution was the result of at least five runs. Intensities were plotted as a function of the copolymer concentration (% w/v) and the CMC was established as the intersection between the two straight lines.

2.4.2. Size, size distribution and Z-potential

The hydrodynamic diameter (D_h), the size distribution (polydispersityindex, PDI) and the Z-potential of IDV-free and IDV-loaded PMs were determined using a Zetasizer Nano-ZS (see above), at 37 °C. The Z-potential was measured by laser Doppler microelectrophoresis. Values are expressed as mean ± S.D. of three independent samples prepared under identical conditions. Data for each single specimen were the result of at least five runs.

2.4.3. Visualization and quantification of the polymeric micelles in suspension

The visualization of the polymeric micelles in aqueous dispersion (0.09% w/v) and the subsequent quantification per mL was done by Nanoparticle Tracking Analysis (NTA) in a Malvern NanoSight® NS500-Zeta HSB system with high sensitivity camera and red laser of 638 nm for fluorescent analysis (Malvern Instruments), at 37 °C. The copolymer concentration was initially 0.009% w/v (above the corresponding CMC values) to ensure the formation of micelles and diluted (1:10) in water pre-warmed at 37 °C immediately before the analysis to fit the measurement range of the NTA instrument (10^7–10^9 particles/mL). Due to the shortness of the analysis, no disassembly was expected. Finally, concentration (micelles/mL) values were obtained by multiplying the experimental data by a factor of 10.

2.4.4. Mucoadhesiveness

The mucoadhesiveness of the micelles *in vitro* was estimated by the mucin solution method that is based on the agglomeration of the micelles and the increase of the D_h due to the interaction with mucin [34,35]. For this, mucin was dissolved in acetate buffer pH 5.5 to a final concentration of 0.25% w/v at room temperature. Then, equal volumes of the mucin and polymeric micelles (0.1% w/v) were mixed, vortexed for 30 s and incubated in a thermostated bath (Vicking Masson, Buenos Aires, Argentina) at 37 °C (2 h). The D_h, PDI and Z-potential were followed up and compared to the original micelles. The mucoadhesion index (MI) was calculated according to Eq. (2)

$$\mathrm{MI} = \frac{D_{h2}}{D_{ho}} \tag{2}$$

where D_{h0} D_{h2} are the D_h of particles before (t = 0 h) and after (t = 2 h) the incubation with mucin, respectively. Assays were conducted in triplicate and results are expressed as the mean ± S.D. Data for each single sample were the result of at least five runs. Statistical analysis was conducted by two-way mixed repeated measures analysis of variance (2-way mixed RM ANOVA, significance level of 5%) with Bonferroni post-test for intergroup comparisons, using GraphPad Prism version 6.00 for Windows (GraphPad Software, Inc., USA).

2.4.5. Encapsulation of IDV

The drug-loading capacity of the micelles was assessed using IDV as model hydrophobic drug. In brief, an excess of IDV was poured into a micellar system (5% w/v) and stirred at 37 ± 2 °C for 48 h. Then, the resulting suspensions were filtered (0.45 μm cellulose nitrate membranes, GE Osmonics Inc., Minnetonka, MN, USA) to remove insoluble IDV and a sample (20 μL) was withdrawn for quantification of the IDV payload by high performance liquid chromatography (HPLC) (Waters Corp., Milford, MA, USA). For this, 980 μL of mobile phase was added to the extracted sample, vortexed (45 s), filtered (0.45 μm nylon membranes) and injected in an Alliance separation module e2695 (Waters Corp., Milford, USA) with a Eurospher II C18P column (5 mm, 150 × 4 mm, Knauer, Berlin, Germany) and a UV detector (λ = 210 nm, 2998 Photodiode Array UV–vis 2D detector, W2998). The mobile phase was acetonitrile:triethylammonium buffer pH 6.50 (40:60 v/v) and the injection volume 100 μL. Measurements were conducted at 25 °C using a flow rate of 1 mL/min [33]. IDV concentration was obtained by interpolation of the sample peak area in a calibration curve with linearity over the range of 1–100 μg/mL (R^2 = 0.9997). The solubility factor (f_s) was determined according to Eq. (3)

$$f_s = \frac{S_a}{S_i} \tag{3}$$

where S_a is the apparent solubility of IDV in the micelles and S_i is the intrinsic solubility of IDV in acetate buffer pH 5.50, as established in our laboratory (63 ± 10 μg/mL). Measurements were performed in triplicate and the results are expressed as the mean ± S.D. Statistical analysis was conducted by one-way analysis of variance

Table 1
Chemical and thermal characterization of CS-*g*-PNIPAAm copolymers synthesized with different γ-irradiation doses.

Sample	Irradiation dose (kGy)	%NIPAAm	Char yield (%)[a]	LCST (°C)[b]	T_g (°C)[b]
CS	–	0	0.42	–	–
Poy(NiPAAm)	–	100	1.58	–	165
CS-*g*-PNIPAAm-05	5	57	18.18	32.0	162
CS-*g*-PNIPAAm-10	10	48	14.18	32.2	146
CS-*g*-PNIPAAm-20	20	37	4.22	32.3	140

[a] Char yield (%) is the residual weight after heating to 800 °C under a nitrogen atmosphere, as determined by TGA.
[b] Determined by DSC.

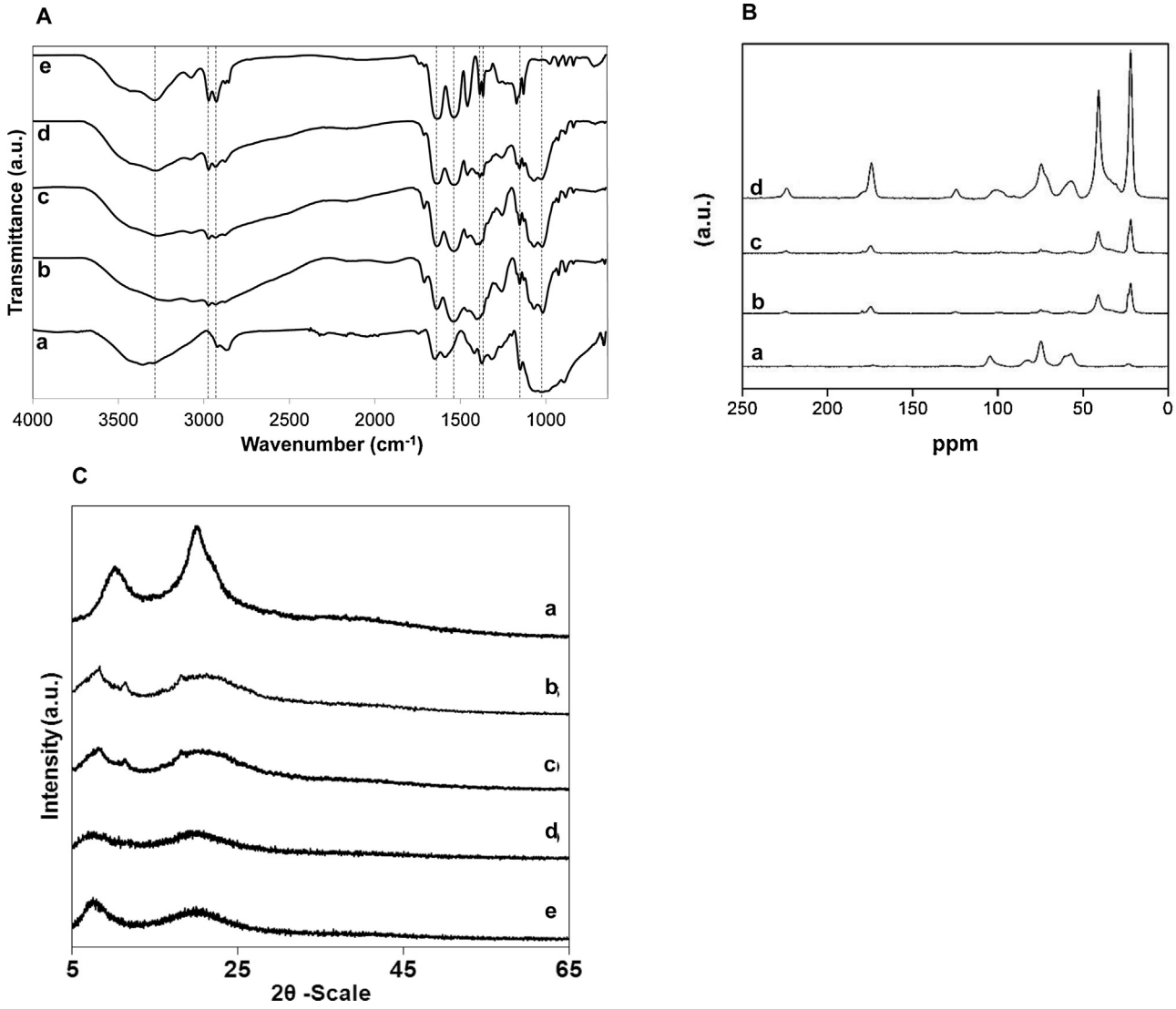

Fig. 1. Characterization of the CS-*g*-PNIPAAm copolymers synthesized by a one-pot γ-radiation-assisted pathway. (A) FTIR-ATR spectra of (a) CS, (b) CS-*g*-PNIPAAm-05, (c) CS-*g*-PNIPAAm-10, (d) CS-*g*-PNIPAAm-20 and (e) PNIPAAm homopolymer. (B) ^{13}C NMR spectra of (a) CS, (b) CS-*g*-PNIPAAm-05, (c) CS-*g*-PNIPAAm-10 and (d) CS-*g*-PNIPAAm-20. (C) X-ray diffraction pattern of (a) CS, (b) CS-*g*-PNIPAAm-05, (c) CS-*g*-PNIPAAm-10, (d) CS-*g*-PNIPAAm-20 and (e) PNIPAAm homopolymer.

(ANOVA, significance level of 5%) with Newman–Keuls post-test for intergroup comparisons, using GraphPad Prism version 6.00.

3. Results and discussion

3.1. γ-Radiation-assisted synthesis and chemical characterization of CS-g-PNIPAAm copolymers

Three copolymers with different NiPAAm weight content were obtained by changing the radiation dose (Table 1). A priori, two binding sites in the CS backbone could be anticipated; the C-2 amine groups of deacetylated units and the hydroxyl groups on C-3 and C-6 carbons on acetylated or deacetylated units of CS (Scheme 1), as described elsewhere [36]. However, the medium and catalysts can direct the reaction to the former or the latter, respectively. For example, under acid conditions and without catalyst, the amine groups are the primary reaction site [37]. At the same time, the formation of free radical species along the CS backbone or in the alpha position to primary hydroxyl groups could not be ruled out. The free radical mechanism could also lead to the formation of a free radical in the NIPAAm precursor and the subsequent homopolymerization [38]. In this work, graft copolymers were synthesized in aqueous

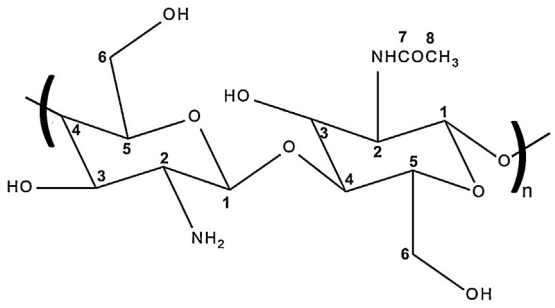

Scheme 1. Chitosan structure.

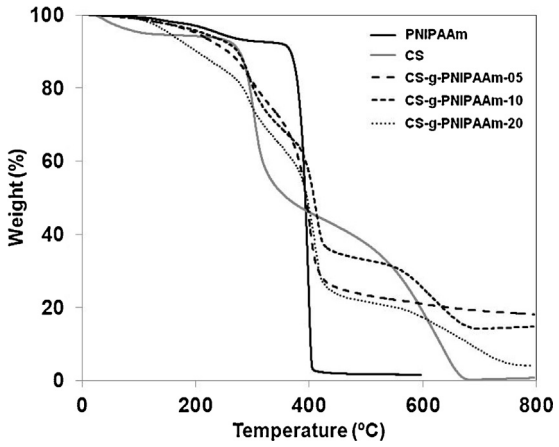

Fig. 2. TGA thermogram of PNIPAAm, CS and three copolymers in the temperature range between 25 and 800 °C.

medium employing different radiation doses, 5, 10 and 20 kGy and without the addition of chemical initiators or catalysts (Table 1). The different copolymers were yellow to orange solids that dissolved well in water. The grafting of PNIPAAm was confirmed by ATR-FTIR (Fig. 1A). Pure CS exhibited characteristic absorption bands at 3355 (overlapping of O—H and N—H stretching bands), 2870 (stretching of C—H), 1591 (bending of N—H), 1150 (stretching of C—O—C in glycosidic linkage) and 1025 cm^{-1} (stretching of C—O—C in glucosamine) (Fig. 1A,a, Supplementary Table 1). A band at 1648 cm^{-1} also confirmed its partial deacetylation, as reported by the supplier. In PNIPAAm, absorption bands at 3287, 1634 and 1538 cm^{-1} were assigned to the presence of the amide group and a doublet at 1387 and 1367 cm^{-1} to the isopropyl group (Fig. 1A,e, Supplementary Table 1) [39]. The graft copolymers showed the typical bands of both PNIPAAm and CS at 1635–1639, 1553–1554, 1150 and 1018–1026 cm^{-1} (Fig. 1A,b–d, Supplementary Table 1). These results were in good with the literature [40]. The band at 1591 cm^{-1} belonging to the N—H bending of primary amines in the spectrum of CS was very weak, suggesting that, the grafting occurred mainly in the free amine groups [37]. At the same time, since the intensity of these bands is weak, other grafting sites could not be ruled out (see below). In addition, the gradual decrease of the relative intensity of band at 1538 cm^{-1} from CS-*g*-PNIPAAm-05 to CS-*g*-PNIPAAm-20 was consistent with a decrease of the graft polymerization and an increase of the homopolymerization pathway as the dose increased.

The grafting of PNIPAAm blocks in the different copolymers was confirmed by ^{13}C CP/MAS NMR spectroscopy. CS showed characteristic signals at 57.08 ppm (C2), 60.14 ppm (C6), 74.68 ppm (C3/C5), 82.16 ppm (C4) and 104.52 ppm (C1) (Fig. 1B,a) [41,42]. Signals for carbonyl group at 173.37 ppm (C7) and methyl group at 22.97 ppm (C8) were also observed because the deacetylation extent was not 100%. The copolymers displayed several new peaks in the ranges of 10–50 and 170–182 ppm that were assigned to aliphatic and carbonyl signals of the PNIPAAm blocks, respectively (Fig. 1B,b–d), as reported elsewhere [40]. In addition, the relative signals of CS gradually decreased with respect to those of PNIPAAm as the dose increased.

Once the grafting was confirmed qualitatively, the analysis focused on the quantification of the grafting yield and the%NIPAAm. ^{1}H NMR data showed that the % NIPAAm of CS-PNIPAAm-05, CS-*g*-PNIPAAm-10 and CS-*g*-PNIPAAm-20 was 57%, 48% and 37% w/w, respectively (Table 1). These findings indicated that for higher radiation doses, the secondary homopolymerization pathway was more prominent and were in very good agreement with ATR-FTIR and ^{13}C NMR analyses.

3.2. Powder X-ray diffraction

The diffractogram of CS showed two major peaks at 2θ 10.06° and 19.98° that belong the most ordered region in the molecule involving the acetamide groups [43]. PNIPAAm homopolymer presented a completely amorphous structure. CS-PNIPAAm-05, CS-*g*-PNIPAAm-10 and CS-*g*-PNIPAAm-20 showed a NIPAAm-like diffraction pattern (Fig.1C).

3.3. Thermal stability of CS-g-PNIPAAm copolymers

TGA analysis aimed to evaluate the effect of the grafting on the thermal stability of CS. The thermogram of CS exhibited two distinct degradation stages. The first at approximately 300 °C due to a complex process including dehydration of sugar rings, depolymerization and decomposition of acetylated and deacetylated units (Fig. 1). The second transition at ~640 °C was assigned to the total degradation of the polymer [44,45]. Conversely, PNIPAAm homopolymer presented a single degradation stage at 398 °C (Fig. 2). Instead, the decomposition temperature of CS and PNIPAAm in the copolymers was lower and higher than that of each individual homopolymer, respectively. Moreover, the thermal stability of the copolymers increased with respect to the individual components (Table 1). Thus, CS and NIPAAm homopolymers resulted in 0.42% and 1.58% char yield, respectively, while the copolymers where in the 4.22–18.88% range; the higher the % NIPAAm, the lower the char yield. In any event, since these thermal changes take place at extremely high (and physiologically irrelevant) temperatures, the performance of the different copolymers under physiological conditions will not be affected.

3.4. Thermal transition and T_g of NIPAAm blocks in the copolymers

The thermal behavior of the grafted PNIPAAm blocks will govern the ability of the copolymers to self-assemble in aqueous medium. Thus, dry samples were wetted with a small volume of water, and analyzed by DSC between 20 and 200 °C at a very low heating rate (1 °C/min). The first endothermic transition corresponded to the LCST that was approximately at 32 °C, irrespective of the grafting extent (Fig. 3A, Table 1). This value was consistent with results reported for other PNIPAAm-grafting systems [46–48]. Moreover, the thermal transition was clearly visualized as the transformation of a translucent solution into an opalescence dispersion (Fig. 3B). At higher *T*, a second transition due to the T_g of PNIPAAm blocks at 140–162 °C was apparent (Table 1). These values coincided with the value shown by PNIPAAm homopolymer at 165 °C. CS-*g*-PNIPAAm-20 showed the weakest transition and at the lowest *T* due to the lower PNIPAAm content.

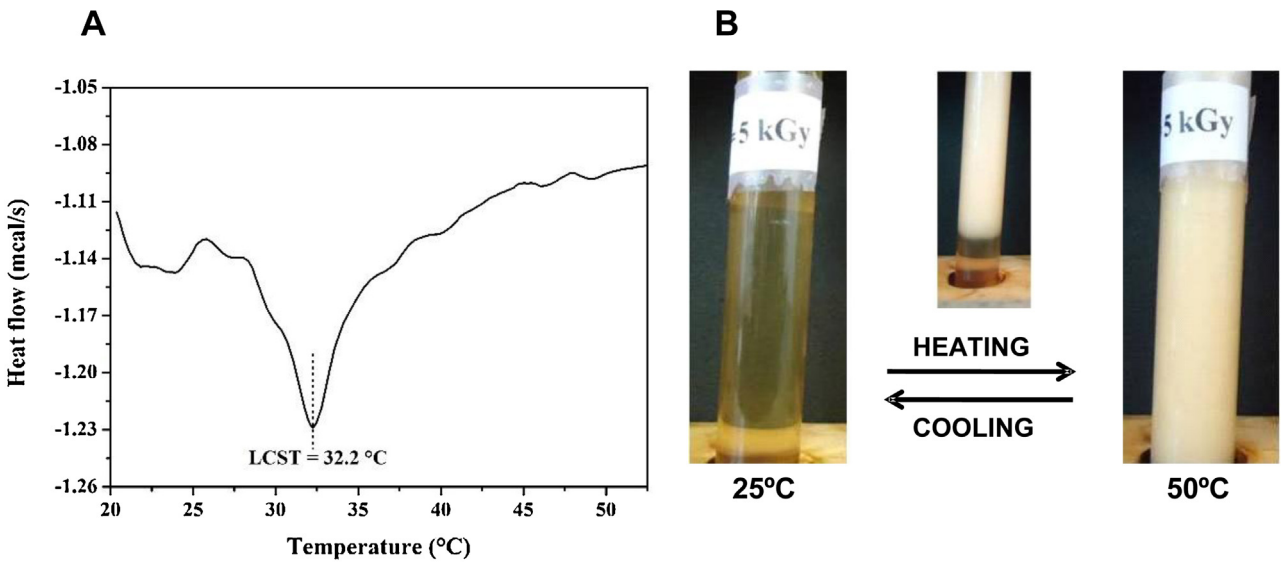

Fig. 3. Thermal transition of CS-*g*-PNIPAAm-05 upon heating. (A) DSC thermogram showing the transition endotherm at 32.2 °C that belongs to the lower critical solution temperature (LCST) and (B) change in the appearance of a 1% w/v copolymer solution at temperatures below and above the LCST.

3.5. Preparation and characterization of CS-g-PNIPAAm micelles

3.5.1. CMC and micellar size, size distribution and Z-potential

The hydrophobization of CS with PNIPAAm blocks was undertaken to grant it aggregation properties. However, since the LCST of PNIPAAm is 32 °C, the copolymers were fully hydrophilic below this critical temperature because water molecules form hydrogen bonds with the polar groups of PNIPAAm (amide group), masking their hydrophobic *N*-isopropyl groups [49,50]. In this context, the copolymers undergo aggregation only at temperatures above the LCST and consequently, the CMC was measured at 37 °C. Below the CMC, the intensity of scattered light detected for each sample was similar to that obtained with the acetic acid solution pH 5.50. Once reached the CMC, the sample scattering intensity increased linearly with the concentration (Supplementary Fig. 1). Usually, the scattering intensity in DLS increases with the size of the aggregates. Intriguingly, the size of the structures at 37 °C decreased upon micellization (Supplementary Fig. 1). These findings might suggest more complex aggregation patterns and a transition from a non- or partly aggregated and expanded larger molecular array below the CMC, to a more compact and smaller one above it. Current investigations are being devoted to elucidate the phenomena taking place.

CS-*g*-PNIPAAm-05, CS-*g*-PNIPAAm-10 and CS-*g*-PNIPAAm-20 showed CMC values of 0.0012, 0.0019 and 0.0025% w/v that were consistent with the chemical characterization, where a greater radiation dose led to copolymers with lower %NIPAAm and HLB (Table 2). Considering that the volume of fluids in the gastrointestinal tract vary between 300 and 500 mL for the fasting state and 800–1000 mL for the fed state [51], the low value of CMC obtained with any of the copolymers suggested that the micelles would withstand the dilution in the gastrointestinal tract [52]. In addition, above the CMC (0.01% w/v), the size of the micelles stabilized at a relatively constant value (Supplementary Fig. 1). The higher the PNIPAAm content, the larger the size (Table 2); D_h values being 202, 115 and 100 nm for CS-*g*-PNIPAAm-05, CS-*g*-PNIPAAm-10 and CS-*g*-PNIPAAm-20, respectively, at 37 °C. At a substantially higher concentration (5% w/v), the size followed a similar trend, though with a sharp increase to 1254, 459 and 289 nm for graft copolymers produced with growing radiation dose.

The D_h is governed by structural features of both the corona and the core; the relative content of CS determines the contribution of the corona to the size, while the content of PNIPAAm has a similar effect on the core. The PMs of this work showed a gradual decrease of the D_h with the decrease of the %PNIPAAm (Table 2). These findings suggested that the size was more influenced by the hydrophobic component and that the higher the %PNIPAAm, the larger the core and the larger the micelle. It is worth stressing that all the micelles showed a relatively low PDI that was in accordance with monomodal size distributions and Z-potential values between +15.0 and +24.6 mV that indicated the availability of protonated free amine groups (Table 2). These findings were in good agreement with FTIR data, where a decrease in the intensity of the amine group band was apparent upon NiPAAm grafting, indicating that these groups were partly involved in the reaction.

3.5.2. Visualization and quantification of the polymeric micelles

To gain further insight into the behavior of the micelles though in suspension, the novel NTA was used to analyze samples of the different copolymers at a concentration that was above the CMC of all the copolymers (0.009% w/v) and at the same time in the measurement range of the instrument. A fast dilution method was used to comply with both conditions (see experimental section). The visualization is presented in the Supplementary videos. The concentration of micelles decreased from 17.3×10^9 micelles/mL for CS-*g*-PNIPAAm-20 to 1.5×10^9 for CS-*g*-PNIPAAm-10 (Table 2). These two graft copolymers displayed similar CMC and a slight increase of micellar size for the derivative with greater %NiPAAM, suggesting that CS-*g*-PNIPAAm-20 (the most hydrophilic derivative) generates a larger amount of smaller micelles (100 nm) than the more hydrophobic CS-*g*-PNIPAAm-20 that gave place to a smaller number of larger micelles (115 nm) (Table 3). Conversely, the most hydrophobic copolymer of the series, CS-*g*-PNIPAAm-05, showed the highest concentration, 21.3×10^9 micelles/mL. This phenomenon could be attributed to the fact that the micellization tendency was substantially favored by the even higher hydrophobicity of this copolymer. In addition, the larger size would stem from the generation of a more bulky core due to the greater NIPAAm content.

3.5.3. Mucoadhesiveness

The mucoadhesiveness of the different micelles was evaluated by DLS. It was expected that if the micelles conserved the intrinsic mucoadhesive properties of CS that stem from the presence of free

Table 2
Critical micelle concentration (CMC), hydrodynamic diameter (D_h) and polydispersity index (PDI) values of the different CS-*g*-PNIPAAm copolymers.

Copolymer		D_h (nm) (± S.D.)		PDI (±S.D.)		Z-potential (mV)	Micellar concentration (10^9 micelles/mL)[a] (±S.D.)
	CMC (% w/v)	0.1%	5%	0.1%	5%	0.1%	
CS-*g*-PNIPAAm-05	0.0012	203 (3)	1254 (58)	0.102 (0.032)	0.587 (0.048)	+24.6 (0.6)	21.3 (0.1)
CS-*g*-PNIPAAm-10	0.0019	115 (2)	459 (19)	0.138 (0.026)	0.238 (0.007)	+18.6 (0.8)	1.5 (0.1)
CS-*g*-PNIPAAm-20	0.0025	100 (4)	389 (12)	0.160 (0.011)	0.160 (0.009)	+15.0 (0.7)	17.3 (0.5)

[a] Determined in a sample with initial polymer concentration of 0.009% w/v that was diluted immediately before analysis (1:10) to fit the concentration range of the NTA instrument and corrected by a dilution factor of 10.

Table 3
D_h, PDI and Z-potential of 0.1% w/v polymeric micelles incubated with 0.25% w/v mucin (2 h), at 37 °C.

Sample	Micelles + mucin[a]			
	D_h (nm) (±S.D.)	PDI (± S.D.)	Z-potential (mV) (±S.D.)	MI
CS-*g*-PNIPAAm-05	332* (10)	0.139 (0.012)	+3.9** (1.3)	1.64
CS-*g*-PNIPAAm-10	198* (5)	0.210 (0.011)	+2.8** (0.9)	1.72
CS-*g*-PNIPAAm-20	163* (10)	0.674 (0.051)	+4.4** (1.6)	1.63

* Statistically significant increase of the micellar size after 2 h incubation with mucin with respect to the initial micellar size ($p < 0.05$).
** Statistically significant decrease of the micellar Z-potential after 2 h incubation with mucin with respect to the initial Z-potential ($p < 0.05$).
[a] Mucin dispersion showed a bimodal distribution with D_h values of 86 ± 21 nm (83.9% of intensity) and 586 ± 48 nm (16.1% of intensity) and PDI of 0.488 ± 0.081 and Z-potential of −9.3 ± 0.8 mV.

Table 4
Hydrodynamic diameter (D_h), apparent solubility (S_a) and solubility factor (f_s) of IDV-loaded micelles. The micellar concentration was 5% w/v.

Copolymer	IDV loaded micelles			
	D_h (nm) (±S.D.)	PDI (±S.D.)	S_a (μg/mL) (±S.D.)	f_s (±S.D.)
CS-*g*-PNIPAAm-05	1579 (23)	0.699 (0.046)	N.D.	N.D.
CS-*g*-PNIPAAm-10	412 (21)	0.160 (0.009)	1213* (152)	19.2 (2.4)
CS-*g*-PNIPAAm-20	355 (12)	0.029 (0.033)	1446* (50)	22.9 (0.8)

N.D.: not determined.
* Statistically significant increase of the S_a with respect to the intrinsic solubility of IDV in buffer pH 5.5, 63 ± 10 μg/mL ($p < 0.05$).

amine groups and hydrophilic and hydrophobic domains, mucin molecules would promote their aggregation, increasing their D_h and changing their surface charge (Z-potential).

Mucin dispersions are highly polydisperse in size. Indeed, at pH 5.50 and 37 °C, they showed two size populations with D_h of 86 ± 21 and 586 ± 48 nm, respectively. When the mucin dispersion was put in contact with the PMs, the peaks of mucin disappeared owing to a molecular redistribution around the micelle and the micellar size significantly increased (Table 3). These results indicated that regardless of the grafting, the PMs remained mucoadhesive to a certain extent. In addition, the Z-potential value of mucin at pH 5.50 was negative, −9.3 ± 0.8 mV due to the presence of sialic acid residues along the backbone. When the micelles were incubated with mucin, a clear decrease of the Z-potential from highly (+15.0 to +24.6 mV) to slightly positive values between +2.8 and +4.4 mV was observed due to the neutralization of the positive charges in CS by the electrostatic interaction with the negatively charged mucin (Table 3). MI values of 1.63–1.72 confirmed the agglomeration of the micelles in the presence of the main component of mucus without a significant effect of the hydrophobicity of the copolymer.

3.5.4. Nano-encapsulation of IDV

To evaluate the nano-encapsulation capability of the PMs, IDV was selected as a hydrophobic model drug. This antiretroviral was part of the therapeutic cocktail until the early 2000s. Regardless of the fact that it was included in 18th World Health Organization (WHO) List of Essential Medicines published in 2013 [53], nowadays, it is only used in second-line treatments in developing countries due to resistance and severe renal side effects [54,55]. IDV presents a relative high molecular mass (613.79 g/mol). In previous studies, the encapsulation of IDV was assessed in polymeric micelles of linear and branched poly(ethylene oxide)-*b*-poly(propylene oxide) copolymers(2) with only a slight solubility increase of up to 3-fold for 10% w/v micellar systems (unpublished results). In these assays, copolymer concentrations were significantly above the CMC (5% w/v) to ensure the presence of micelles.

Encapsulation of IDV within CS-*g*-PNIPAAm-05 micelles led to a significant enlargement of the polymeric micelles to 1579 nm that precluded the filtration to remove insoluble drug (Table 4). Thus, the apparent solubility in the micelles could not be determined accurately. Conversely, the size of CS-*g*-PNIPAAm-10 and CS-*g*-PNIPAAm-remained almost unchanged and with a slight size decrease to 412 and 355 nm, respectively. Accordingly, the solubility increased from 63.2 μg/mL to 1.21 and 1.45 mg/mL for CS-*g*-PNIPAAm-10 (f_s = 19.1) and CS-*g*-PNIPAAm-20 (f_s = 22.9) micelles, respectively (Table 4). The substantially greater encapsulation extent with respect to conventional polymeric micelles produced with amphiphilic triblocks (*e.g.*, poloxamers) and even using a lower concentration would most probably stem from the dramatically lower CMC and more complete aggregation of these graft copolymers in water that leads to the formation of more micelles able to incorporate a hydrophobic cargo.

4. Conclusions

PNIPAAm blocks were successfully grafted to CS templates using a one-step γ-radiation pathway. The amount of PNIPAAm and CS was controlled by total dose. The copolymers underwent a thermo-sensitive self-assembly process in water at relatively low concentrations. Moreover, the polymeric micelles retained mucoadhesive properties of CS and encapsulated the bulky poorly water-soluble IDV molecule. Overall results converge to support the potential of this very versatile strategy that can combine different multifunctional polymers and hydrophobic blocks to

extend the role of these nanocarriers to mucosal drug applications.

Acknowledgments

This work was supported by the European Union's—Seventh Framework Programme under grant agreement #612675-MC-NANOTAR, DGAPA-UNAM (Grant IN200714) and CONACYT-CNPq (Grant 174378). Authors thank the "Red iberoamericana de nuevos materiales para el diseño de sistemas avanzados de liberación de fármacos en enfermedades de alto impacto socioeconómico" (RIMADEL) of the Ibero-American Programme for Science, Technology and Development (CYTED) during the period 2011-2014 and the technical assistance of M. Cruz and E. Palacios (ICN-UNAM) and A. Tejeda (IIM-UNAM).

Appendix A. Supplementary data

Supplementary data associated with this article can be found, in the online version, at http://dx.doi.org/10.1016/j.colsurfb.2015.10.036.

References

[1] K. Kataoka, A. Harada, Y. Nagasaki, Adv. Drug Deliv. Rev. 64 (2012) 37.
[2] D.A. Chiappetta, A. Sosnik, Eur. J. Pharm. Biopharm. 66 (2007) 303.
[3] L. Bromberg, J. Control. Release 128 (2008) 99.
[4] G. Gaucher, P. Satturwar, M.-C. Jones, A. Furtos, J.-C. Leroux, Eur. J. Pharm. Biopharm. 76 (2012) 147.
[5] C. Alvarez-Lorenzo, A. Sosnik, A. Concheiro, Curr. Drug Targets 12 (2011) 1112.
[6] H. Cabral, K. Kataoka, J. Control. Release 190 (2014) 465.
[7] A. Sosnik, M. Menaker Raskin, Biotechnol. Adv. 33 (2015) 1380.
[8] T. Keana, M. Thanou, Adv. Drug Deliv. Rev. 62 (2010) 3.
[9] M.J. Alonso, A. Sanchez, J. Pharm. Pharmacol. 55 (2003) 1451.
[10] R.A.A. Muzzarelli, C. Muzzarelli, Adv. Polym. Sci. 186 (2005).
[11] M. Jayukumar, P.T. Prabaharan, S.V. Nair, H. Tamura, Biotechnol. Adv. 29 (2011) 322.
[12] A. Sosnik, J. das Neves, B. Sarmento, Prog. Polym. Sci. 39 (2014) 2030.
[13] I.A. Sogias, A.C. Williams, V.V. Khutoryanskiy, Biomacromolecules 9 (2008) 1837.
[14] B. Menchicchi, J.P. Fuenzalida, K.B. Bobbili, A. Hensel, M.J. Swamy, F.M. Goycoolea, Biomacromolecules 15 (2014) 3550.
[15] J. Smith, M. Dornish, E.J. Wood, Pharm. Res. 21 (2004) 43.
[16] T.H. Yeh, L.W. Hsu, M.T. Tseng, P.L. Lee, K. Sonjae, Y.C. Ho, H.W. Sung, Biomaterials 32 (2011) 6164.
[17] L. González-Mariscal, P. Nava, S. Hernández, J. Membr. Biol. 207 (2005) 55.
[18] M.A. Deli, Biochim. Biophys. Acta Biomembr. 1788 (2009) 892.
[19] R.J. Glisoni, S. Quintana, M. Molina, M. Calderon, A.G. Moglioni, A. Sosnik, J. Mater. Chem. B 3 (2015) 4853.
[20] A. Sosnik, G. Gotelli, G.A. Abraham, Prog. Polym. Sci. 36 (2011) 1050.
[21] C. Alvarez-Lorenzo, E. Bucio, G. Burillo, A. Concheiro, Expert Opin. Drug Del. 7 (2010) 173.
[22] G. Gurdag, S. Sarmad, Polysaccharide Based Graft Copolymers, in: S. Kalia, M.W. Sabaa (Eds.), Springer-Verlag, Berlin-Heidelberg, 2013, pp. 15–57.
[23] M.H. Casimiro, M.L. Botelho, J.P. Leal, M.H. Gil, Radiat. Phys. Chem. 72 (2005) 731.
[24] D. Singh, V. Choudhary, V. Koul, J. Appl. Polym. Sci. 104 (2007) 145.
[25] Z. Ajji, I. Othman, J.M. Rosiak, Nucl. Instr. Meth. Phys. Res. B 229 (2005) 375.
[26] L. Zhao, H.-J. Gwon, Y.-M. Lim, Y.-C. Nho, S.Y. Kima, Radiat. Phys. Chem. 106 (2015) 404.
[27] K. Qiu, K. Park, Adv. Drug Deliv. Rev. 53 (2001) 321.
[28] B. Jeong, S.W. Kim, Y.H. Bae, Adv. Drug Deliv. Rev. 64 (2012) 154.
[29] Z. Tang, Y. Akiyama, T. Okano, J. Polym. Sci. Part B: Polym. Phys. 52 (2014) 917.
[30] F.M. Winnik, Polymer 31 (1990) 2125.
[31] S. Chee, I. Soutar, L. Swanson, Polymer 42 (2001) 5079.
[32] N. Nagaoka, A. Safraj, M. Yoshida, H. Omichi, H. Kubota, R. Katakai, Macromolecules 26 (1993) 7386.
[33] J.C. Imperiale, P. Nejamkin, M.J. Del Sole, C. Lanusse, A. Sosnik, Biomaterials 37 (2015) 383.
[34] J. Thongborisute, H. Takeuchi, Int. J. Pharm. 354 (2008) 204.
[35] J. das Neves, M.F. Bahia, M.M. Amiji, B. Sarmento, Expert Opin. Drug Del. 8 (2011) 1085.
[36] N.M. Alves, J.F. Mano, Int. J. Biol. Macromol. 43 (2008) 401.
[37] D.V. Luyen, D.M. Huong, Polymeric Materials Encyclopedia, in: J.C. Salamone (Ed.), CRC, New York, 1996, pp. 1208–1215.
[38] J.-P. Wang, Y.-Z. Chen, S.-J. Zhang, H.-Q. Yu, Bioresour. Technol. 99 (2008) 3397.
[39] H. Tu, C.E. Heitzman, P.V. Braun, Langmuir 20 (2004) 8313.
[40] M.K. Jaiswal, R. Banerjee, P. Pradhan, D. Bahadur, Colloids Surf. B 81 (2010) 185, http://dx.doi.org/10.1016/j.colsurfb.2010.07.009.
[41] R. Yoksan, M. Akashi, S. Biramontri, S. Chirachanchai, Biomacromolecules 2 (2001) 1038.
[42] H. Cai, Z.P. Zhang, P.C. Sun, B.L. He, X.X. Zhu, Radiat. Phys. Chem. 74 (2005) 26.
[43] B.A.V. Kumar, M.C. Varadaraj, R.N. Tharanathan, Biomacromolecules 8 (2007) 566.
[44] C. Peniche-Covas, W. Arguelles-Monai, J. San Román, Polym. Degrad. Stab. 39 (1993) 21.
[45] M. Sahin, N. Kocak, G. Arslan, H. Ucan, J. Inorg. Organomet. Polym. 21 (2011) 69.
[46] E. Bucio, E. Arenas, G. Burillo, Mol. Cryst. Liq. Cryst. 447 (2006) 203.
[47] F. Muñoz-Muñoz, J.C. Ruiz, C. Alvarez-Lorenzo, A. Concheiro, E. Bucio, Radiat. Phys. Chem. 81 (2012) 531.
[48] F. Muñoz-Muñoz, E. Bucio, B. Magariñoz, C. Alvarez-Lorenzo, A. Concheiro, J. Appl. Polym. Sci. 131 (2014), Art. 39992.
[49] J. Han, K. Wang, D. Yang, J. Nie, Int. J. Biol. Macromol. 44 (2009) 229.
[50] N.A. Peppas, J. Zhang, Encyclopedia of Biomaterials and Biomedical Engineering, in: G.E. Wnek, G.L. Bowlin (Eds.), Dekker, New York, NY, 2006, pp. 1–9.
[51] A. Dahan, G. Amidon, In: H. van de Waterbeemd, B. Testa (Eds.). Wiley-VCH Verlag, Berlin-Heidelberg. pp. 33–51, 2009.
[52] H. Wei, X.-Z. Zhang, Y. Zhou, S.-X. Cheng, R.-X. Zhuo, Biomaterials 27 (2006) 2028.
[53] WHO.18th World Health Organization (WHO) List of Essential Medicines (Final amendments October 2013). http://www.who.int/medicines/publications/essentialmedicines/en.
[54] M. Boyd, Expert Opin. Pharmacother. 8 (2007) 957.
[55] T. Bunupuradah, T. Puthanakit, P. Fahey, A. Kariminia, N.K.N. Yusoff, T.H. Khanh, A.H. Sohn, K. Chokephaibulkit, P. Lumbiganon, R. Hansudewechakul, K. Razali, N. Kurniati, B.V. Huy, T. Sudjaritruk, N. Kumarasam, S.M. Fong, V. Saphonn, J. Ananworanich, TApHOD, Antivir. Ther. 18 (2013) 591.